In situ observation of the ferroelectric-paraelectric phase transition in a triglycine sulfate single crystal by variable-temperature electrostatic force microscopy

E. Z. Luo,* Z. Xie, J. B. Xu, and I. H. Wilson
Department of Electronic Engineering and the Materials Science & Technology Research Center, The Chinese University of Hong Kong, New Territories, Hong Kong, People's Republic of China

L. H. Zhao
Applied Physics Department, Hunan University, Changsha 410082, People's Republic of China

(Received 15 June 1999)

The ferroelectric-paraelectric phase transition of triglycine sulfate single crystal was investigated by variable-temperature electrostatic force microscopy. Near the Curie temperature T_C, the evolution of ferroelectric domains with temperature was observed *in situ*. We have found that the domain structures are not thermally reversible until $T_C-2\,^\circ\mathrm{C}<T<T_C$, within which the domain density N diverges reversibly via $(T_C-T)^{-\eta}$, with $\eta=0.54\pm0.05$, larger than is predicted by mean-field theory. The spontaneous polarization P in individual domains decreases continuously and reversibly to zero and eventually vanishes at T_C. Quantitative analysis reveals that $P^2\propto(T_C-T)$.

I. INTRODUCTION

Triglycine sulfate [TGS:$(NH_2CH_2COOH)_3H_2SO_4$] is a well-known ferroelectric material and is of special interest because it is one of the few ferroelectric crystals having typically a second-order phase transition (ferroelectric-paraelectric) at its Curie point T_C (49 °C).[1–4] Below the Curie point TGS exists as a typical uniaxial ferroelectric phase, the spontaneous polarization P is along the crystallographic b axis with antiparallel 180° configurations. The most interesting issue in a second-order phase transition is the critical phenomena near T_C.[1–4] Macroscopic measurements have proved that the material can be well described by Landau's mean-field theory.[5,6] The critical behavior of the order parameter is Landau type with the critical exponent $\beta=\frac{1}{2}$, i.e.,

$$P\propto\tau^{\beta}\ \ (T<T_C), \tag{1}$$

where $\tau=(T_C-T)/T_C$ is the reduced temperature. Another interesting phenomenon in a second-order phase transition is domain evolution with temperature. The critical behavior of the equilibrium domain density N can be written as[1–4]

$$N\propto\tau^{-\eta}\ \ (\eta=\tfrac{1}{4},\ \ T<T_C). \tag{2}$$

The exponent $\eta=\frac{1}{4}$ has rarely been measured. By using nematic liquid-crystal method, Nakatani measured the temperature dependence of domain width, which is the inverse of N, in TGS during cooling down from above T_C.[7] The thermodynamic reversibility was not studied in Ref. 7. From the data presented in Ref. 7, one can calculate that η is close to 1 when T is very close to T_C. Similar results have also been observed by Wang *et al.* in $La_{1-x}Nd_xP_5O_{14}$ (LNPP) single crystals,[8] which exhibit a strong thermal hyteresis effect in domain density. However, it decreases rapidly as T deviates from T_C. Therefore, from both experimental and theoretical points of view, it is highly desirable to visualize *in situ* the domain evolution during the phase transition on a nanometer scale. It is also of great interest to experimentally verify the phenomenological mean-field theory at the single domain scale. This demands a technique with capability of imaging ferroelectric domains with high resolution and in an environment with high-temperature stability and accuracy.

Significant progress has been achieved in imaging domains in ferroelectric single crystals and thin films by using various forms of scanning force microscopes (SPM's),[9] including conventional atomic force microscopy (AFM),[10] lateral force microscopy (LFM),[11,12] and electrostatic force microscopy (EFM) in contact and noncontact mode.[13–16] Recently, Hong and co-workers pointed out that EFM working in dynamic contact mode (they term it DC-EFM) has superior domain contrast to that by noncontact EFM.[17,18] There have been some observations of domain evolution in TGS.[11,13,17] However, little attention has been paid to thermodynamics. In this paper, we present a study of the ferroelectric-paraelectric phase transition of TGS by using DC-EFM. For this purpose, we have designed a special heating stage with high-temperature stability and accuracy.[19] By controlling the sample temperature carefully, the temperature dependence of domain configuration, as well as of the spontaneous polarization P in domains, has been studied.

II. EXPERIMENT

The experiments were carried out in a commercial AFM (Nanoscope III, Digital Instruments). A TiN coated tip was used. Here the basic principle of DC-EFM is introduced below. An ac modulation $V=V_{ac}\cos(\omega t)$ was applied between the conducting tip and the bottom electrode of the sample. The ω component of electrostatic force F_e induced by the surface charge is given by[18]

$$F_e(\omega)=(\sigma_b C/2\varepsilon_0)V_{ac}\cos(\omega t), \tag{3}$$

where σ_b is the bounded surface charge density, in the case of ferroelectric domains $\sigma_b=P$, ε_0 is the dielectric constant in vacuum, and C is the tip-sample capacitance. The EFM works in contact mode. Therefore the electrostatic force is proportional to σ_b and V_{ac}. The electrostatic force is detected by a lock-in amplifier and imaged simultaneously with

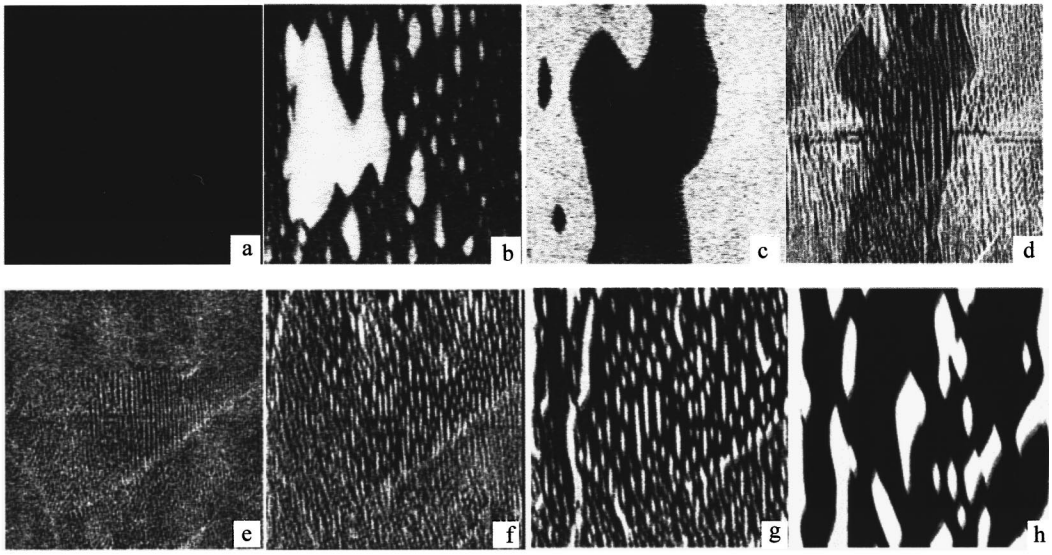

FIG. 1. A series of surface charge images ($40\times40\ \mu$m) on the same sample region in the course of phase transition. Bright and dark regions correspond to positive and negative domains. For heating up, the temperatures are (a): 35 °C; (b): 44.4 °C; (c): 46.5 °C; and (d): 48.2 °C, respectively. For cooling down, (e): 49 °C (T_C); (f): 48.1 °C; (g): 47.7 °C; and (h): 46.7 °C.

surface morphology. From Eq. (3), the image signal V is proportional to P if V_{ac}, the loading force, and other experimental parameters are kept constant. Therefore not only can the domain be imaged but also the spontaneous polarization P can be quantitatively determined provided that the system is calibrated. The DC-EFM used in this study is similar to that described by Ref. 18. In this study, V_{ac} and ω were fixed (2.1 V and 10 kHz) for all temperatures. Temperature signal was either read by a multimeter or fed (through a low noise amplifier) to one of the data channels in the Nanoscope III. Therefore the temperature fluctuation during scanning can be ''imaged'' simultaneously with domain images. A 1-mm thick single TGS crystal was cleaved perpendicularly to the b axis without further treatment. All images presented below were obtained with the same tip and the same loading force, which was estimated to be about 10 nN (not calibrated).

III. RESULTS

At room temperature, the cleaved TGS single crystal exhibits large domains, usually larger than $50\times50\ \mu$m. Figure 1 shows a series of domain images as the temperature was varied through T_C. Figures 1(a)–1(d) correspond to heating and Figs. 1(e)–1(h) to cooling. All images were from the same sample region. The initial state of this region was a single negative domain [Fig. 1(a)]. The bright and dark areas correspond to positive and negative domains, respectively. In order to carry out the experiments as close to thermal equilibrium as possible, a waiting time of more than 10 min was observed before imaging. This ensures that the domain configuration was stable at that temperature. The sample was heated or cooled very slowly, usually at less than 0.4 °C/h in the low-temperature range and less than 0.2 °C/h when the temperature was close to T_C. The temperature ''image'' was taken as an indicator of temperature stability. The temperature fluctuation was always less than 0.07 °C during imaging. The absolute value of T_C was not accurately calibrated. We define the temperature at which Fig. 1(e) was taken as corresponding to T_C (49 °C) since Fig. 1(e) shows the coexistence of a paraelectric phase with very faint ferroelectric domains in the central part of the image. The temperature relative to T_C was calibrated with accuracy better than 0.05 °C. The critical size of domains is about 200 nm from Fig. 1(e).

Figure 1 reveals two important microscopic features of the phase transition. Generally, the domain configuration is irreversible for heating and cooling, in terms of domain morphology and density (Fig. 1). Figure 2 shows the temperature variation of domain wall density N for heating and cooling. When the sample was heated up, small domains with opposite sign nucleated homogeneously at about 40 °C, resulting in a rapid increase of domain density. At about 44 °C, small domains started to coalesce into large ones accompanied by a decrease of domain density until T reached about 47 °C, as

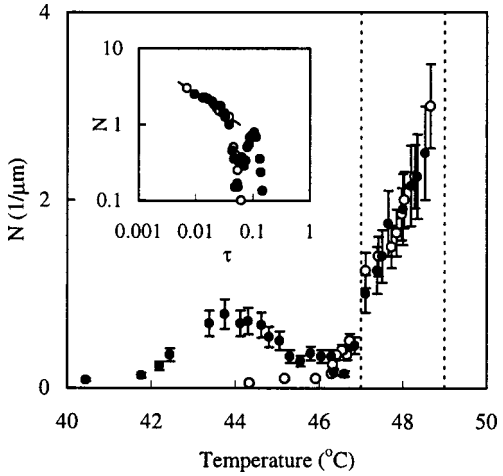

FIG. 2. Temperature variation of domain density N (filled circles: heating; open circles: cooling). Inset: double logarithm plot of N and the reduced temperature τ. The solid line is the fit which gives $\eta=0.55\pm0.05$. The two dashed lines represent $T=47$ and 49 °C, respectively.

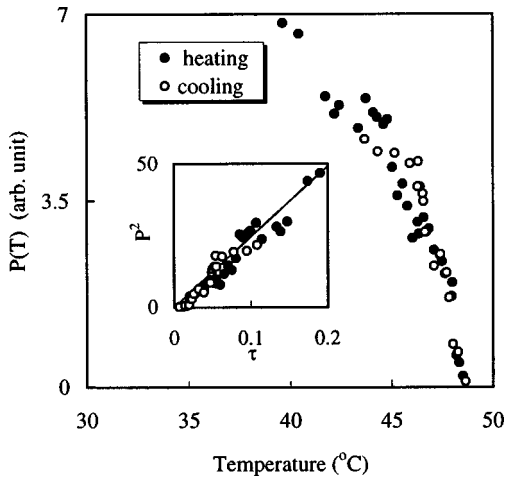

FIG. 3. Spontaneous polarization P vs temperature T, inset: P^2 vs τ plot. The solid line is calculated by using $P^2=A\tau$; A is a constant.

shown in Fig. 2. When T was further increased, N increased drastically again until $T=T_C$. However, when the sample was cooled down from above T_C, positive and negative (P_+ and P_-) domains nucleated periodically and homogeneously. P_+ and P_- domains grew with different speeds as the temperature decreased. Eventually the negative domains (in the example of Fig. 1) dominated the whole image as the temperature was further decreased. During cooling down, the domain density decreased monotonically with decreasing temperature. Figure 2 reveals also that when $T>47\,^\circ\mathrm{C}=T_C-2\,^\circ\mathrm{C}$, N is reversible. Therefore the irreversibility of domain density occurred when $T<T_C-2\,^\circ\mathrm{C}$. Double logarithm N vs τ plot in the inset of Fig. 2 indicates $N\propto\tau^{-\eta}$, shown by the solid line, and $\eta=0.54\pm0.05$. Here only the data within the reversible range have been taken for fitting. The measured η is larger than the theoretical value of 0.25. The kink in the N vs τ plot was also observed by Nakatani.[7]

Second, it is also interesting to note the signal amplitude in the domain images. As mentioned above, the image signal (brightness and darkness of respective domains) measures the polarization P. In order to show this quantitatively, image statistics were performed. Figure 3 shows the temperature variation of average polarization P in single domains [here $P=(|P_+|+|P_-|)/2$] to smooth the slight random asymmetry of P_+ and P_- occurring occasionally). As shown by Fig. 3, P decreases continuously to zero as T approaches T_C, revealing the nature of second-order phase transition. Unlike the case of domain density shown in Fig. 2, here $P(T)$ is reversible (within the error of experiments) throughout the whole temperature range. The inset of Fig. 3 is the P^2 vs τ plot; the straight line is calculated according to Eq. (1). The data are quite scattered, which could originate from a number of factors such as electronic noise, temperature fluctuations, etc. Therefore, taking Fig. 3 as guidance, it is reasonable to conclude that our results have verified the mean-field theory experimentally at the single domain scale.

IV. DISCUSSION

By using a temperature variable EFM, not only the domain evolution during phase transition has been directly visualized, but also the domain density N and polarization P have been obtained quantitatively. The critical behavior of the respective quantities has been studied. On the microscopic scale, the phase transition is characterized by two steps. Massive formation of domains with opposite polarity (this occurs at about 40 °C) and disappearance of domains at T_C. In the thermally reversible regime, $N\propto\tau^{-\eta}$, where the measured $\eta=0.54$ is larger than the theoretical value of 0.25. One of the most crucial experimental errors is the uncertainty of T_C, since this affects the fitting of η as well as β significantly. Actually, if T_C were manually shifted by 0.5 °C in fitting, one would obtain $\eta=0.3$. However, it seems unlikely that the error of T_C was as much as 0.5 °C in our experiments, otherwise β will deviate 0.5 by a large amount. In practice, the domain structures are easily affected by the experimental conditions, especially by the conductivity of the sample and environment.[20,21] Since as T approaches T_C, the domain-wall energy goes to zero, any fluctuation will influence the domain structure. Therefore more experiments (e.g., carry out the experiments in vacuum) are needed to clarify this point. The massive nucleation of domains at 40 °C and the irreversibility of domain structures for $T<T_C-2\,^\circ\mathrm{C}$ agree qualitatively well with macroscopic measurements using the internal friction method.[8,22]

In conclusion, by using a temperature variable EFM, the domain evolution of triglycine sulfate single crystal during the ferroelectric-pyroelectric phase transition near T_C was observed *in situ* and several aspects of the critical phenomena have been studied in detail. The domain structure is thermally reversible only if $T_C-2\,^\circ\mathrm{C}<T<T_C$. The equilibrium domain density diverges via $(T_C-T)^{-\eta}$ and the value of the critical exponent $\eta=0.55\pm0.05$ has been determined (larger than the theoretical value of 0.25). On the single domain scale, $P^2\propto(T_C-T)$ is valid, therefore Landau's mean-field theory has been experimentally verified on a nanometer scale.

ACKNOWLEDGMENTS

We are grateful for Prof. N. Nakatani, who has provided us the TGS single crystal. This work has been in part supported by Hong Kong RGC through projects: CUHK5041/95E and CUHK4175/98E. The authors thank Professor N. Nakatani and Professor W. L. Zhong for valuable discussions and carefully reading the manuscript. We also thank Professor Y. H. Xu and Dr. X. R. Wang for their valuable discussions.

*Electronic address: ezluo@ee.cuhk.edu.hk

[1] M. E. Lines and A. M. Glass, *Principles and Application of Ferroelectric and Related Materials* (Oxford University Press, Oxford, 1977).

[2] W. L. Zhong, *Physics of Ferroelectrics* (Scientific, Beijing, 1996) (in Chinese).

[3] B. A. Strukov and A. P. Levanyuk, *Ferroelectric Phenomena in Crystals* (Springer-Verlag, Berlin, 1998).

[4] Y. H. Xu, *Ferroelectric Materials and their Applications* (North-Holland, Amsterdam, 1991).
[5] J. A. Gonzalo, Phys. Rev. **144**, 622 (1966).
[6] M. Mierzwa, B. Fugiel, and K. Cwikiel, J. Phys.: Condens. Matter **10**, 8881 (1998).
[7] N. Nakatani, Jpn. J. Appl. Phys., Part 2 **24**, L528 (1985).
[8] Y. N. Wang, W. Y. Sun, X. H. Chen, H. M. Shen, and B. S. Lu, Phys. Status Solidi A **102**, 279 (1987).
[9] R. Luehi, H. Haefke, K. P. Meyee, E. Meyer, L. Howald, and H. J. Guenterodt, J. Appl. Phys. **74**, 7461 (1993).
[10] S. Balakumar, J. B. Xu, I. H. Wilson, G. Arunmozhi, N. Nakatani, and T. Yamazaki, Jpn. J. Appl. Phys., Part 1 **46**, 4377 (1997).
[11] A. Correia, J. Massanell, N. Garcia, A. P. Levanyuk, A. Zlatkin, and P. Przeslawski, Appl. Phys. Lett. **68**, 2796 (1996).
[12] H. Bluhm, U. D. Schwarz, and R. Wiesendanger, Phys. Rev. B **57**, 161 (1998).
[13] R. Luethi, H. Haefke, W. Gutmannsbauer, E. Meyer, L. Howald, and H. J. Guetherodt, J. Vac. Sci. Technol. B **12**, 2451 (1994).
[14] M. Abplanalp, L. M. Eng, and P. Guenter, Appl. Phys. A: Mater. Sci. Process. **66A**, S231 (1998).
[15] A. Gruverman, H. Tokumoto, A. S. Prakash, S. Aggarwal, B. Yang, M. Wuttig, R. Ramesh, O. Auciello, and T. Vehkastesan, Appl. Phys. Lett. **71**, 3492 (1997).
[16] G. Zavala, J. H. Fendler, and S. Trolier-Mckinstry, J. Appl. Phys. **81**, 7480 (1997).
[17] J. W. Hong, K. H. Noh, Sang-il Park, S. I. Kwun, and Z. G. Kim, Phys. Rev. B **58**, 5078 (1998).
[18] J. W. Hong, Sang-il Park, and Z. G. Kim, Rev. Sci. Instrum. **70**, 1735 (1999).
[19] Z. Xie, E. Z. Luo, J. B. Xu, and I. H. Wilson (unpublished).
[20] N. Takanani, Ferroelectrics **97**, 127 (1989).
[21] N. Takanani (private communication).
[22] Z. M. Liu, X. H. Chen, H. M. Shen, Y. N. Wang, H. F. Young, and P. C. W. Fung, Phys. Status Solidi A **116**, K199 (1989).